

# Parameter Estimation using Maximum Likelihood Method from Flight Data at High Angles of Attack

Rakesh Kumar and A. K. Ghosh

## I. INTRODUCTION

THE estimation of aerodynamic parameters from real flight data is a routine task for many aerospace organizations. Parameter estimation [1-4] is the process of determining the best possible estimates of the aerodynamic parameters occurring in the model used to represent it. Under stationary attached flow conditions, aerodynamic effects are adequately described using time-invariant parameters and linear models. After a priori fix of the aerodynamic model used, the next task of estimating parameters is, generally, attempted by three different techniques: analytical methods, wind-tunnel methods and flight-test methods. At initial stages of aircraft design, analytical methods [3] provide the only convenient way of estimating the aircraft parameters. Since such theoretical estimates may have low accuracy level, there is a need to verify these estimates with those obtained from wind tunnel and flight tests.

At higher angles of attack (aircrafts undergoing stall), the models are highly nonlinear due to dominant unsteady effects due to flow separation. Unsteady aerodynamics [5-7] has been a subject of extensive investigations using computational fluid dynamic methods, wind tunnel tests and semi-empirical models. Although such models provide a basis for analytical investigations of the complex flow phenomena, but postulating them in an analytical form suitable for parameter estimation is difficult. An alternative approach [5] to describe the flow separation analytically including stall hysteresis as a function of an internal state variable has been followed in the present study. Since the approach retains the state-space formulation, it is directly amenable to identification and validation from flight data [6-7].

In this paper, the Kirchhoff's model (quasi-steady stall) using the Maximum-Likelihood method [3] has been applied to the longitudinal aerodynamic data generated through flight testing to capture nonlinear aerodynamics of Hansa-3 aircraft.

An approach of fixing the strong parameters close to their wind tunnel values was followed during the estimation of quasi-steady stall characteristics and the longitudinal aerodynamic parameters from flight data pertaining to quasi-steady stall maneuver (QSSM).

The procedure to generate real flight data by flight testing of Hansa-3 aircraft and data compatibility check are described in the section entitled 'Longitudinal Aerodynamic Data: Hansa-3 aircraft'. Quasi-steady stall modeling is outlined in the next section followed by the application of the models to the real flight data and discussion of the results. Concluding remarks are presented at the end of the paper.

**Abstract**—The paper presents the modeling of nonlinear longitudinal aerodynamics using flight data of Hansa-3 aircraft at high angles of attack near stall. The Kirchhoff's quasi-steady stall model has been used to incorporate nonlinear aerodynamic effects in the aerodynamic model used to estimate the parameters, thereby, making the aerodynamic model nonlinear. The Maximum Likelihood method has been applied to the flight data (at high angles of attack) for the estimation of parameters (aerodynamic and stall characteristics) using the nonlinear aerodynamic model. To improve the accuracy level of the estimates, an approach of fixing the strong parameters has also been presented.

**Keywords**—Maximum Likelihood, nonlinear, parameters, stall.

## NOMENCLATURE

A	Aspect ratio
$a_1$	Static stall characteristics parameter
$a_x, a_y, a_z$	Longitudinal, lateral and vertical components of acceleration, $m/s^2$
$b$	Wing span, m
$C_D, C_L, C_m$	Drag, lift and pitching moment coefficients
$C_{D_0}, C_{L_0}, C_{m_0}$	Drag, lift and pitching moment coefficients at zero angle of attack
$\bar{c}$	Mean aerodynamic chord, m
$m$	Mass, kg
$p, q, r$	Angular rates (roll, pitch and yaw), rad/s
$\dot{p}, \dot{q}, \dot{r}$	Rates of angular rates, $rad/s^2$
S	Reference area, $m^2$
T	Temperature, $^{\circ}C$
t	Time, s
$u, v, w$	Components of velocity along x, y and z-body axes, m/s
X	Instantaneous location of an idealized flow separation point along chord on the upper surface of the wing
$X_0$	Steady flow separation point
$\alpha, \beta$	Angle of attack and sideslip, rad
$\alpha^*$	Break point corresponding to $X_0=0.5$
$\delta_a, \delta_e, \delta_r$	Deflections of aileron, elevator and rudder, rad
$\Theta, \xi$	Vectors of unknown parameters
$\square, \theta, \psi$	Angles of roll, pitch and yaw, rad
$\tau_1$	Transient time constant
$\tau_2$	Quasi-steady time constant

Rakesh Kumar is Assistant Professor in Aerospace Engineering Department at PEC University of Technology, Chandigarh, India (phone: +91-9878215676; fax: +91-512-2597561; e-mail: rakpec@iitk.ac.in).

A. K. Ghosh is Professor in Aerospace Engineering Department at Indian Institute of Technology, Kanpur, India (e-mail: akgh@iitk.ac.in).

## II. LONGITUDINAL FLIGHT DATA: HANSA-3 AIRCRAFT

A flight test program was carried out at the Indian Institute of Technology, Kanpur to obtain the real flight data of Hansa-3 aircraft (Fig. 1). The linear and the nonlinear flight data were generated corresponding to 3-2-1-1 (moderate angles of attack) and quasi-steady stall maneuver (high angles of attack) using elevator control input.

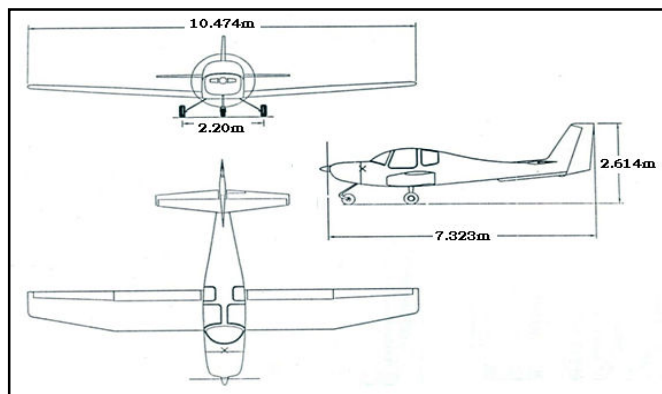


Fig. 1 Planform of Hansa-3 aircraft

The mass and geometric characteristics of Hansa-3 aircraft are shown in Table I. The elevator from trim condition was deflected by the pilot to execute 3-2-1-1 and quasi-steady stall maneuver (QSSM). However, the execution of 3-2-1-1 maneuvers was not difficult as the control deflections were limited to generate the response of motion variables at moderate angles of attack, but the execution of quasi-steady stall maneuver was not an easy task as the control deflection involved high angles of attack near stall. In spite of a lot of efforts, only one set of flight data corresponding to quasi-steady stall maneuver, that reasonably represented the nonlinear characteristics, could be generated.

TABLE I  
 MASS AND GEOMETRIC CHARACTERISTICS OF H-3 AIRCRAFT

Component (symbol)	Value (units)
Aircraft mass ( $m$ )	750 kg
Wing planform area ( $S$ )	12.47 m <sup>2</sup>
Aspect ratio ( $A$ )	8.8
Mean aerodynamic chord ( $\bar{c}$ )	1.21 m
Root chord ( $C_r$ )	1.3 m
Tip chord ( $C_t$ )	0.8 m
Span ( $b$ )	10.47 m
Taper ratio ( $\lambda$ )	0.8
Planform area of horizontal tail ( $S_t$ )	2.04 m <sup>2</sup>
Mean chord of horizontal tail	0.59 m

An onboard measurement system installed on the test aircraft provided the measurements using dedicated sensors such as aircraft motion variables, atmospheric conditions, control surface deflections, etc. The measurements made in flight were recorded on board at a sampling rate of 50 Hz using suitable interface with the standard Laptop using virtual instrumentation. The raw flight data for  $V$ ,  $\alpha$ ,  $\beta$ ,  $p$ ,  $q$ ,  $r$ ,  $a_x$ ,  $a_y$ ,  $a_z$ ,  $\phi$ ,  $\theta$ ,  $\psi$ ,  $h$ ,  $\delta_a$ ,  $\delta_e$  and  $\delta_r$  were measured. The measurements

of speed ( $V$ ), angle of attack ( $\alpha$ ) and angle of sideslip ( $\beta$ ) were obtained with flight log mounted on a boom fixed to the tip of the wing.

The accelerations ( $a_x$ ,  $a_y$ ,  $a_z$ ) along the three body axes were measured using an accelerometer located near the centre of gravity of the aircraft. The angular rates ( $p$ ,  $q$  and  $r$ ) were obtained from the measurements available from the inertial platform. The rates of angular rates ( $\dot{p}$ ,  $\dot{q}$  and  $\dot{r}$ ) were obtained by numerical differentiations of the corresponding angular rates. The control deflections ( $\delta_a$ ,  $\delta_e$  and  $\delta_r$ ) were measured using potentiometer. The temperature  $T$  was recorded using standard cockpit outside air temperature (OAT) gauge.

After establishing a typical cruise at desired speed and altitude, the elevator was deflected to excite longitudinal dynamics of Hansa-3 aircraft using 3-2-1-1 (Fig. 2) and quasi-steady stall maneuver (Fig. 3).

Figure 2 presents the variation of angle of attack ( $\alpha$ ), pitch angle ( $\theta$ ), pitch rate ( $q$ ), velocity ( $V$ ) and acceleration along x- and z-axis ( $a_x$  and  $a_z$ ) for 3-2-1-1 elevator control input. The variables  $\alpha$ ,  $\beta$ ,  $\phi$ ,  $\theta$ ,  $\psi$  and  $\delta_e$  used in various plots are in degrees whereas the variables  $a_x$  and  $a_z$  are in m/s<sup>2</sup>. The variables  $V$ ,  $h$  and  $q$  are in m/s, m and deg/s, respectively. It can be observed from Fig. 2 that the negative elevator deflection (trailing edge deflected upwards) from trim condition leads to increase in  $\alpha$ ,  $\theta$ ,  $q$ ,  $a_x$  (a measure of drag) and  $a_z$  (a measure of lift) whereas the trend of variation gets reversed when the deflection is in opposite direction. The velocity reduces as the elevator is deflected in negative direction (3-2-1-1 input) and increases as the elevator is deflected in positive direction from trim condition.

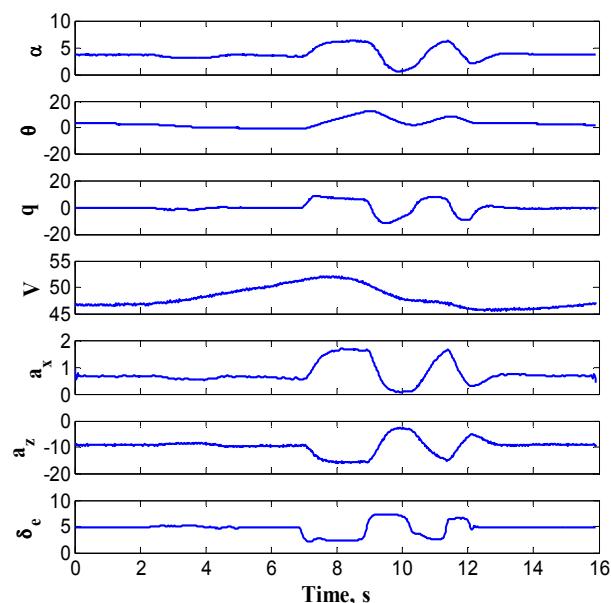


Fig. 2 Real flight data at moderate A.O.A.: 3-2-1-1 input

Figure 3 presents the variation of real flight data motion variables with time for the quasi-steady stall maneuver. It can be observed from Fig. 3 that the maximum angle of attack ( $\alpha$ ) of 18 degrees has been achieved by the execution of quasi-steady stall maneuver using elevator control ( $\delta_e$ ). The sudden change in the value of vertical acceleration ( $a_z$ ), considered as

a measure of the lift, confirms a drop in the lift coefficient beyond the angle of attack of 18 degrees. The drop in  $C_L$  beyond 18 degrees establishes the occurrence of stall phenomena. The acceleration ( $a_x$ ) along x-body axis, considered as a measure of the drag, indicates that the drag increases drastically during the stall. All other variables vary in a manner as the execution of such quasi-steady stall maneuver. The pitch angle ( $\theta$ ) dips and even touches -18 degrees during the maneuver. Similarly, the sudden change in pitch rate ( $q$ ) is observed near the stall region. The speed ( $V$ ) of aircraft keeps on increasing as long as the pitch angle keeps on decreasing.

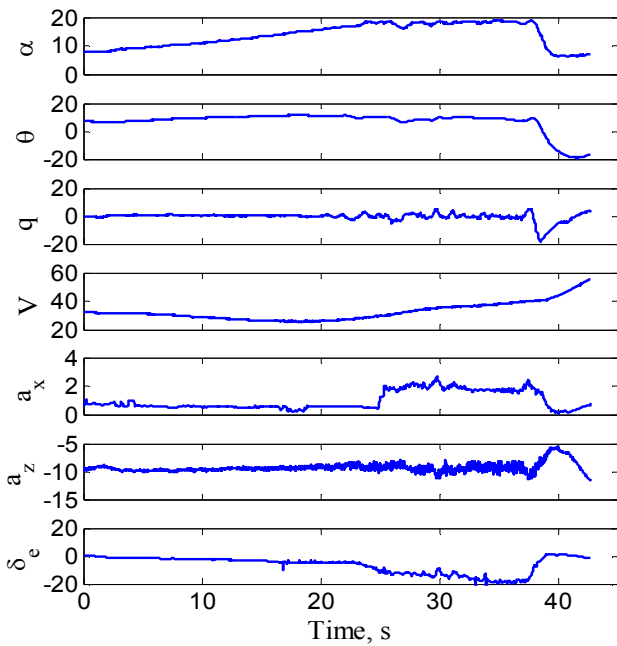


Fig. 3 Real flight data at high angles of attack: QSSM

Next, data compatibility check also referred to as Flight Path Reconstruction (FPR) was carried out on both of the real flight data to ensure that the measurements used for subsequent aerodynamic model identification were consistent and error free. The scale factors and biases present in the measured flight variables were estimated using observation equations and the ML algorithm. The following set of unknown parameters was considered adequate for reconstructing the longitudinal dynamics of Hansa-3 aircraft.

$$\Theta = [\Delta a_x \Delta a_y \Delta a_z \Delta p \Delta q \Delta r K_\alpha \Delta \alpha K_\beta \Delta \beta]^T \quad (1)$$

The measured and computed response of motion variables obtained during data compatibility check are presented in Figs. 4 and 5 for 3-2-1-1 input and QSSM, respectively. It can be observed that a reasonably good match of measured and computed responses of motion variables such as  $V$ ,  $\alpha$ ,  $\beta$ ,  $\phi$ ,  $\theta$ ,  $\psi$  and  $h$  are obtained.

The estimated compatibility factors obtained during the data compatibility check using the ML method are given in Table 2. The real flight data is assumed to be of good quality if the estimated values of biases and scale factors come out to be negligible and close to unity, respectively. It can be observed from Table 2 that the values of biases are negligible and scale

factor is close to unity in case of 3-2-1-1 control input. Since the quasi-steady stall maneuver (QSSM) encounters large sideslip angles, the values of scale factor ( $K_\beta$ ) and bias ( $\Delta\beta$ ) for sideslip angle were also estimated. It can be observed from Table 2 that the values of biases such as  $\Delta a_y$ ,  $\Delta a_z$ ,  $\Delta\beta$ ,  $\Delta p$ ,  $\Delta q$  and  $\Delta r$  are negligible whereas the value of bias,  $\Delta a_x$ , is slightly higher. The values of scale factors  $K_\beta$  and  $K_\alpha$  depart from unity. This departure may be due to inappropriate attitude of vanes during the execution of quasi-steady stall maneuver.

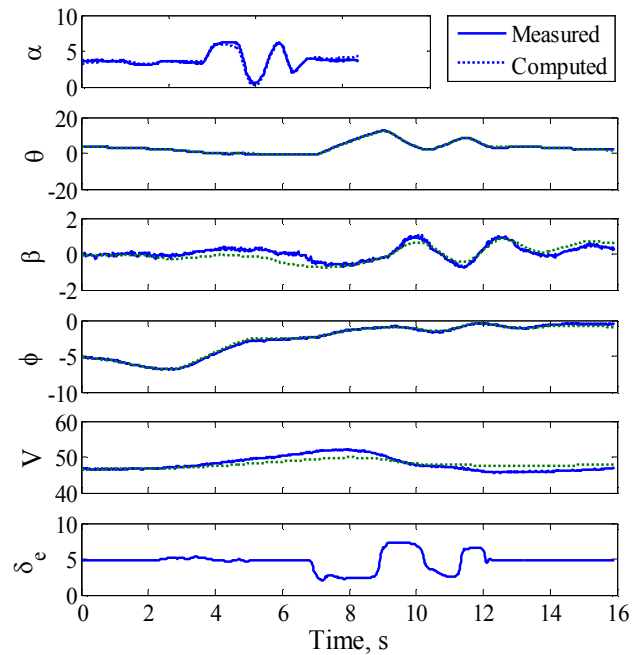


Fig. 4 Measured and computed variables during FPR; 3-2-1-1 input

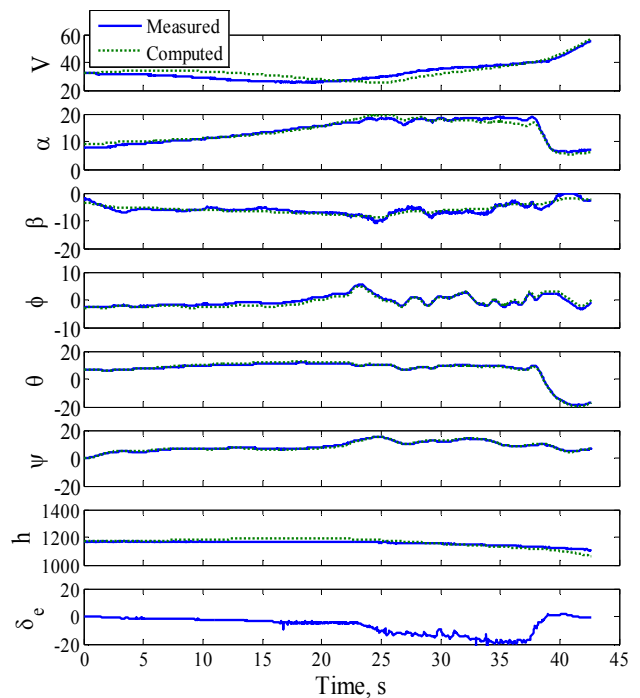


Fig. 5 Measured and computed variables during FPR; QSSM

TABLE II  
COMPATIBILITY FACTOR DURING DATA COMPATIBILITY CHECK

Input	3-2-1-1	QSSM
$\Delta a_x$ (m/s <sup>2</sup> )	0.080 (0.080)	-0.82 (0.003)
$\Delta a_y$ (m/s <sup>2</sup> )	-0.026 (0.001)	-0.045 (0.002)
$\Delta a_z$ (m/s <sup>2</sup> )	0.011 (0.0)	-0.025 (0.0)
$\Delta p$ (rad/s)	-0.0007 (0.0)	-0.0008 (0.0)
$\Delta q$ (rad/s)	-0.001 (0.0)	-0.0004 (0.0)
$\Delta r$ (rad/s)	0.003 (0.0)	0.0048 (0.0)
$K_\beta$ (-)	-	0.3 (0.003)
$\Delta\beta$ (rad)	-	-0.051 (0.001)
$K_\alpha$ (-)	1.02 (0.008)	0.627 (0.003)
$\Delta\alpha$ (rad)	-0.004 (0.0)	0.119 (0.001)

( ) Cramer-Rao bounds

### III. QUASI-STEADY STALL MODELING

Aerodynamic models become highly nonlinear due to dominant unsteady effects due to flow separation at high angles of attack for aircraft undergoing stall. For such a case, based on Kirchhoff's theory of flow separation for a symmetrical profile, the lift coefficient can be modeled as a function of  $\alpha$  and steady-state flow separation point<sup>(3)</sup>:

$$C_L(\alpha, X) = C_{L\alpha} \left\{ \frac{1+\sqrt{X}}{2} \right\}^2 \alpha \quad (2)$$

Reformulating the Kirchhoff formulation of separated flow lift (2) and extending it by  $C_{L_0}$  for non-symmetrical profile yields the following expression [3] for steady state of flow separation point  $X_0$ .

$$X_0 = \left\{ 2 \sqrt{[(C_L - C_{L_0}) / (C_{L\alpha} \alpha)] - 1} \right\}^2 \quad (3)$$

The steady flow separation point ( $X_0$ ) depends upon the airfoil and wing configuration. Using Eq. (2) with  $X=X_0$  the function can be determined statically in wind tunnel by substituting the values of  $C_{L\alpha}$ ,  $C_{L_0}$  and  $C_L$  obtained through wind tunnel testing. It may be noted that the values of  $C_{L\alpha}$  required in (3) corresponds to linear value of the lift curve slope for the presented work in this paper. An alternative procedure has been used in this work wherein  $X_0$  has been modeled as per (4).

$$X_0 = \frac{1}{2} \{1 - \tanh [a_1(\alpha - \alpha^*)]\} \quad (4)$$

where  $a_1$  defines the static stall characteristics of the airfoil and  $\alpha^*$  the breakpoint corresponding to  $X_0 = 0.5$ . Equation (4) represents the steady-state stall model for steady-state flow separation point as a function of  $a_1$  and  $\alpha^*$ . This approximation is better suited to parameter estimation because it is a continuous function in its entire range and has just two unknown parameters, namely  $a_1$  and  $\alpha^*$ .

The above information is suitable for steady-state stall modeling of  $C_L$  as a function of  $\alpha$  and steady-state flow separation point  $X_0$ . However, aircraft in actual case of dynamic motion requires the formulation of the flow separation point. The representation of expression characterizing transient and quasi-steady effects is given by:

$$\tau_1 \frac{dX}{dt} + X = \frac{1}{2} \{1 - \tanh [a_1(\alpha - \tau_2 \dot{\alpha} - \alpha^*)]\} \quad (5)$$

The flight maneuvers containing adequate information was required to estimate the parameters ( $a_1, \alpha^*, \tau_1$  and  $\tau_2$ ) appearing in the model defined by (5). Estimation of  $\tau_1$  and  $\tau_2$  requires dynamic stall maneuvers. Quasi-steady stall maneuvers can be performed more easily in stead of risky dynamic stall to gather the nonlinear flight data. Therefore, a simplified approach accounting for quasi-steady stall characteristics ( $a_1, \alpha^*$  and  $\tau_2$ ) as recommended in Ref. (3) has been used. Flight data with quasi-steady stall would enable estimation of the hysteresis time constant  $\tau_2$  only. Accordingly, the transient effects can be neglected by setting  $\tau_1$  to zero. This eliminates the need of the differential equation. Equation (5) can be written as [3]:

$$X = \frac{1}{2} \{1 - \tanh [a_1(\alpha - \tau_2 \dot{\alpha} - \alpha^*)]\} \quad (6)$$

The estimation of parameters  $a_1$  (airfoil stall characteristics),  $\tau_2$  (time constant) and  $\alpha^*$  (break point) are sufficient to adequately model the stall hysteresis.

### IV. RESULTS AND DISCUSSION

The quasi-steady stall model was applied to the real flight data of Hansa-3 aircraft for the estimation of aerodynamic parameters and quasi-steady stall characteristics. The flight dynamic model<sup>(3)</sup> simulating the longitudinal dynamics is given by (7):

$$\dot{\alpha}(t) = q(t) - \frac{\rho V S}{2m} C_L(t) \quad (7a)$$

$$\dot{q}(t) = \frac{\rho V^2 S \bar{c}}{2I_y} C_m(t) \quad (7b)$$

Quasi-steady stall model as given in (6) was used to model the nonlinear unsteady aerodynamics. The linear and the nonlinear aerodynamic models [3] are given in (8) and (9), respectively.

$$C_L = C_{L_0} + C_{L\alpha} \alpha \quad (8a)$$

$$C_D = C_{D_0} + \frac{1}{\pi A} C_L^2 \quad (8b)$$

$$C_m = C_{m_0} + C_{m\alpha} \alpha + C_{m_q} \frac{q\bar{c}}{2V} + C_{m_{\delta e}} \delta e \quad (8c)$$

$$C_L = C_{L_0} + C_{L\alpha} \left\{ \frac{1+\sqrt{X}}{2} \right\}^2 \alpha \quad (9a)$$

$$C_D = C_{D_0} + \frac{1}{\pi A} C_L^2 + \frac{\partial C_D}{\partial X} (1 - X) \quad (9b)$$

$$C_m = C_{m_0} + C_{m\alpha} \alpha + C_{m_q} \frac{q\bar{c}}{2V} + C_{m_{\delta e}} \delta e + \frac{\partial C_m}{\partial X} (1 - X) \quad (9c)$$

where  $A$ ,  $e$ ,  $\delta e$  and  $q$  are the wing aspect ratio, the Oswald factor, elevator deflection and pitch rate, respectively. The empirical correction terms, such as  $\frac{\partial C_D}{\partial X}$  and  $\frac{\partial C_m}{\partial X}$ , model any hysteresis effect in the drag and pitching moment coefficient. The model for flow separation point as given in (6) was used.

The aim was to estimate the parameter vector given in (10).

$$\xi = [a_1 \ \alpha^* \ \tau_2 \ C_{L_0} \ C_{L\alpha} \ C_{D_0} \ \frac{\partial C_D}{\partial X} \ C_{m_0} \ C_{m\alpha} \ C_{m_q} \ C_{m_{\delta e}} \ \frac{\partial C_m}{\partial X}]^T \quad (10)$$

The cost function that was minimized using the ML method to estimate the parameter vector  $\xi$  is given by (11).

$$J(\xi, R) = \frac{1}{2} \sum_{k=1}^N [Z(k) - Y(k)]^T R^{-1} [Z(k) - Y(k)] \quad (11)$$

$$\text{where } R = \frac{1}{N} \sum_{k=1}^N [Z(k) - Y(k)][Z(k) - Y(k)]^T$$

The terms  $R$ ,  $Z(k)$  and  $Y(k)$  are defined as measurement covariance matrix, measured and estimated output vector at  $k^{\text{th}}$  instant, respectively.  $N$  and  $k$  are number of data points and general index for data points, respectively. The ML method was applied to estimate parameter vector  $\xi$  by minimizing the cost function  $J(\xi, R)$ . The estimated values along with the Cramer-Rao bounds were obtained to assess the accuracy of the parameter estimates.

First, the longitudinal aerodynamic parameters ( $C_{D_0}$   $C_{L_0}$   $C_{L_\alpha}$   $C_{m_0}$   $C_{m_\alpha}$   $C_{m_q}$   $C_{m_{\delta_e}}$ ) were estimated from the real flight data pertaining to 3-2-1-1 control input using the linear aerodynamic model and the Maximum Likelihood method. The values of estimated aerodynamic parameters are presented in Table 3. It can be observed that the values of most of the aerodynamic parameters compare well with the wind tunnel values. The values given in parentheses are the Cramer-Rao bounds giving the accuracy level of the estimates.

TABLE III  
PARAMETER ESTIMATION USING ML METHOD

Derivatives (WT values)	3-2-1-1 Input	(QSSM-Aerodynamic parameters fixed)	(QSSM-Stall characteristics fixed)
$C_{D_0}$ (0.035)	0.035 (0.0001)	0.035	0.036 (0.002)
$C_{L_0}$ (0.354)	0.370 (0.0047)	0.37	0.6 (0.007)
$C_{L_\alpha}$ (4.97)	5.00 (0.030)	5.0	4.5 (0.06)
$C_{m_0}$ (0.07)	0.07 (0.0004)	0.07	0.07
$C_{m_\alpha}$ (-0.45)	-0.45 (0.0019)	-0.45	-0.12 (0.01)
$C_{m_q}$ (-8.0)	-8.2 (0.13)	-8.2	-6.3 (1.5)
$C_{m_{\delta_e}}$ (-0.8)	-0.77 (0.005)	-0.77	-0.67 (0.02)
$C_{D_x}$	-	0.042 (0.005)	0.03
$C_{m_x}$	-	-0.20 (0.002)	-0.20
$a_1$	-	33 (1.37)	33
$\tau_2$	-	28 (1.49)	28
$\alpha^*$ (deg)	-	14.8 (0.001)	14.8

( ) Cramer-Rao bounds

During parameter estimation from flight data pertaining to QSSM, most of the parameters were having high correlation with each other which lead to the inaccurate estimation of the parameters when estimated collectively. Therefore, an approach of fixing the strong parameters close to their wind tunnel values was followed. The parameters (aerodynamic and stall characteristics) from nonlinear flight data pertaining to QSSM were estimated in two phases. In first phase, values of aerodynamic parameters ( $C_{D_0}$   $C_{L_0}$   $C_{L_\alpha}$   $C_{m_0}$   $C_{m_\alpha}$   $C_{m_q}$   $C_{m_{\delta_e}}$ ) were fixed to the values obtained through 3-2-1-1 input to estimate stall characteristic parameters ( $a_1$   $\alpha^*$   $\tau_2$   $\frac{\partial C_D}{\partial x}$   $\frac{\partial C_m}{\partial x}$ ). In Table 3, parameters without Cramer-Rao bounds represent fixed parameters whereas the parameters with Cramer-Rao bounds represent the estimated parameters. It was found that the magnitude and sign of estimated stall characteristic parameters followed the desirable trend<sup>(3)</sup>.

In the second phase, the values of estimated stall characteristics from nonlinear flight data pertaining to QSSM were fixed to estimate the longitudinal aerodynamic parameters. Since, the pitching moment coefficient at zero angle of attack ( $C_{m_0}$ ) is a strong derivative, its value was also fixed to 0.07. It can be observed from Table 5 that the magnitude of most of the estimated aerodynamic parameters ( $C_{D_0}$   $C_{L_\alpha}$   $C_{m_q}$   $C_{m_{\delta_e}}$ ) compare well with the wind tunnel values and the values estimated through 3-2-1-1 input. However, the aerodynamic parameters such as  $C_{L_0}$  and  $C_{m_\alpha}$  deviated from the wind tunnel values slightly.

The lower accuracy level of some of the estimates from nonlinear flight data pertaining to QSSM may be attributed to the distorted orientation of the sensors (angle of attack and sideslip vanes) employed to capture the real flight data.

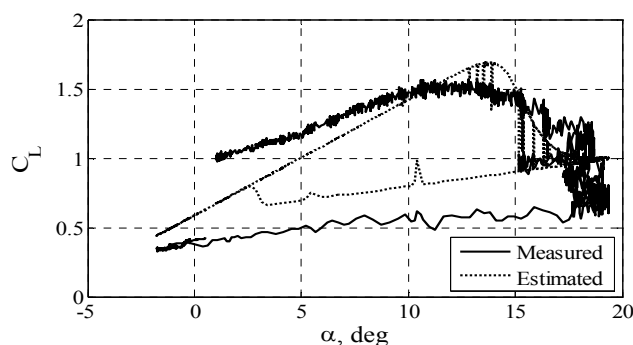


Fig. 6 Measured and estimated stall hysteresis for Hansa-3 aircraft

Figure 6 presents the comparison of stall hysteresis obtained from the real flight data and from the quasi-steady stall model (Eq. 6). It can be observed that the model hysteresis loop fairly well matches with the real flight data hysteresis loop.

## V. CONCLUSION

Quasi-steady stall model was applied to the longitudinal aerodynamic real flight data near stall generated through flight test program of Hansa-3 aircraft. Due to high correlation between the parameters, an approach of fixing the strong parameters close to their wind tunnel values were followed during the estimation of stall characteristics and the longitudinal aerodynamic parameters from the nonlinear flight data pertaining to QSSM.

It was observed that the magnitude of most of the aerodynamic parameters estimated through QSSM compared well with the wind tunnel values. However, some of the aerodynamic parameters deviated from the wind tunnel values slightly.

The lower accuracy level of some of the estimates may be attributed to slightly inappropriate execution of QSSM and the distorted orientation of the sensors (angle of attack and sideslip vanes) employed to capture the real flight data during the execution of QSSM.

All the parameters could not be estimated collectively. Only one set of nonlinear flight data pertaining to QSSM could be gathered in spite of lot of efforts. More accurate real flight data near stall is required to establish the quasi-steady stall model in a better way.

REFERENCES

- [1] Maine, R. E., and Iliff, K. W., "Identification of Dynamic Systems - Application to Aircraft - Part 1: Output Error Approach," AGARD-AG-300, Vol. 3, Part 1, Dec. 1986.
- [2] Greenberg, H., "A Survey of Methods for Determining Stability Parameters of an Airplane from Dynamic Flight Measurements," NACA TN-2340, April 1951.
- [3] Jategaonkar, R. V., *Flight Vehicle System Identification - A Time Domain Methodology*, AIAA Progress in Aeronautics and Astronautics, Vol. 216, AIAA, Reston, VA, Aug 06.
- [4] Kumar, Rakesh and Ghosh, A.K., "Nonlinear Aerodynamic Modeling of Hansa-3 Aircraft using Neural Gauss-Newton Method", Journal of Aerospace Sciences and Technologies, Vol.63, No.3, August, 11
- [5] Goman, M. & Khrabrov, A., "State-space representation of aerodynamic characteristics of an aircraft at high angles of attack," *J. of Aircraft*, Vol. 31, No. 51, 1994.
- [6] Greenwell, D.I., "A Review of Unsteady Aerodynamic Modeling for Flight Dynamics of Manoeuvrable Aircraft," *AIAA Paper*, 2004-5276, 2004.
- [7] Fischenberg, D., "Identification of an Unsteady Aerodynamic Stall Model from Flight Test Data," *AIAA Paper*, 95-3438, 1995.